J. Fluid Mech. (2008), *vol.* 601, *pp.* 189–198.
doi:10.1017/S0022112008000773 Printed in the United Kingdom

A stationary circular hydraulic jump, the limits of its existence and its gasdynamic analogue

ASLAN R. KASIMOV

Department of Mathematics, Massachusetts Institute of Technology, 77 Massachusetts Avenue, Cambridge, MA 02139-4307, USA

(Received 16 October 2007 and in revised form 30 January 2007)

We propose a theory of a steady circular hydraulic jump based on the shallow-water model obtained from the depth-averaged Navier–Stokes equations. The flow structure both upstream and downstream of the jump is determined by considering the flow over a plate of finite radius. The radius of the jump is found using the far-field conditions together with the jump conditions that include the effects of surface tension. We show that a steady circular hydraulic jump does not exist if the surface tension is above a certain critical value. The solution of the problem provides a basis for the hydrodynamic stability analysis of the hydraulic jump. An analogy between the hydraulic jump and a detonation wave is pointed out.

1. Introduction

A hydraulic jump is a phenomenon familiar to everyone – when a water jet from a kitchen tap strikes a horizontal plate, an almost circular ring forms some distance away from the jet impact point. The ring is characterized by a sudden jump in the water depth. The basic problem in the theory of the hydraulic jump is the determination of the jump radius. In this paper we propose a theory for the jump radius that is based on the analysis of the shallow-water equations both upstream and downstream of the jump, paying particular attention to the flow downstream which has not been treated satisfactorily in previous work (see Tani 1949; Watson 1964; Bohr, Dimon & Putkaradze 1993; Bush & Aristoff 2003). We show here that the downstream boundary condition provides a necessary closure that yields a unique unambiguous solution for the jump radius.

We also point out an analogy between the hydraulic jump and a detonation wave, that is a shock wave sustained by the energy released in chemical reactions occurring immediately behind the shock. The analogy stems from a simple observation that both the hydraulic jump and a detonation wave represent shock waves that connect super-critical (supersonic in a detonation wave) flows upstream with subcritical (subsonic in detonations) flows downstream. Just as the jump radius is a principal unknown in the theory of the hydraulic jump, the detonation speed is a principal unknown in detonation theory. The detonation speed is determined by the sonic state downstream of the shock and similarly we demonstrate here that the hydraulic jump radius is also determined by the critical flow condition downstream of the jump. Note that the analogy between a hydraulic jump and a gasdynamic shock wave is well known (see Gilmore, Plesset & Crossley 1950; Stoker 1957; Kate, Das & Chakraborty 2007), but to our knowledge, the analogy we describe here has not been proposed before.

The hydraulic jump has a remarkable history of investigations that starts with the work of Rayleigh (1914), who developed a theory of the jump assuming an inviscid

flow. The assumption turns out to be a rather drastic simplification and leads to results that do not agree with experiment (see Watson 1964). The next major analysis was undertaken 50 years later by Watson (1964), who carefully analysed the structure of the viscous flow in the thin supercritical layer of fluid ahead of the jump and derived a similarity solution of the Navier–Stokes equations. With the velocity profile available, he then imposed the jump conditions on the mass and momentum flux across the hydraulic jump. By assuming the depth after the jump is constant and known, he deduced an expression for the jump radius. Satisfactory agreement with experimental data was found for a laminar hydraulic jump. Despite the apparent success of Watson's theory, it is incomplete since it relies on knowledge of the outer depth of the flow behind the jump. The outer depth should be a part of the solution and as such its determination requires understanding of the flow downstream of the jump and the far-field boundary conditions. Here we emphasize this point on the basis of a simple fact that since the flow after the jump is subcritical, the downstream boundary condition is crucial in the determination of the state just after the jump.

Other notable analytical investigations relevant to our work include those of Tani (1949), Bohr *et al.* (1993) and Bush & Aristoff (2003). Similarly to the approach of Tani (1949), Bohr *et al.* (1993) start with the axisymmetric Navier–Stokes equations and average them in the vertical direction thus obtaining the shallow-water equations for the average radial velocity and fluid depth. The viscous loss terms are approximated based on the average velocity and depth and an ansatz for the vertical velocity profile. By eliminating the depth from the mass and momentum equations they derived an ordinary differential equation for the velocity and then analysed the properties of the solutions of this equation. The equation turns out to have a single critical point which is a spiral (see Tani 1949). Further, they argue that the hydraulic jump occurs near the location of the critical point and from this deduce a scaling law for the radius of the jump. The solutions of the differential equation after the jump were found to blow up at a finite distance, which they assume to be the plate edge.

Bush & Aristoff (2003) modified the analysis of Watson (1964) to include the effects of surface tension in the jump region. Later Bush, Aristoff & Hosoi (2006) experimentally explored the role of surface tension in the instability of the hydraulic jumps as originally reported by Ellegaard *et al.* (1998, 1999). The instability appears in the transition from a circular jump to various polygonal shapes as certain parameters are varied. It was found that the reduction of the surface tension could lead to suppression of the polygonal shapes and transition to a circular jump. It was concluded that the surface tension may be of significance in the onset of polygonal instabilities.

In qualitative agreement with these observations, we find that the inclusion of surface tension leads to a prediction that the steady circular jump does not exist above a certain critical value of the surface tension, implying that a transition to either an unsteady circular jump or a non-circular jump must occur. The dependence of the critical surface tension on viscosity, the flow rate and other parameters of the system can be calculated and, in particular, we show that the critical surface tension decreases with the increase of viscosity, which might explain why the polygonal jumps are observed only in highly viscous fluids. Despite the advances made, however, a satisfactory theoretical explanation of the instability is still lacking. A careful treatment of the base-state steady solution necessary for the stability analysis is one of the goals of the present work.

Section 2 describes the main governing equations together with boundary and jump conditions. In § 3 we analyse the critical points of the differential equation for the flow depth. In § 4 we explain how the jump radius is calculated, and carry out a parametric

analysis exploring the effects of the flow rate, surface tension, viscosity and bottom topography on the jump radius. In § 5 we discuss the results and develop the analogy between the hydraulic jump and a detonation wave in gasdynamics.

2. Governing equations

Following Tani (1949) and adding to his theory the plate-slope function, $s_b(r) = \mathrm{d}b(r)/\mathrm{d}r$, assumed small, with $b(r)$ describing the bottom topography, we arrive at the following boundary-layer approximation of the radial momentum equation:

$$u\frac{\partial u}{\partial r} + v\frac{\partial u}{\partial z} = -g\frac{\mathrm{d}h}{\mathrm{d}r} - gs_b + \nu\frac{\partial^2 u}{\partial z^2}, \tag{2.1}$$

where u and v are the radial (r-axis) and vertical (z-axis) velocity components, h is the fluid depth, g is the constant of gravity, ν is the kinematic viscosity. The equation is subject to the boundary conditions at the plate, $u = v = 0$ at $z = 0$, and at the free surface, $u = U(r)$, $\partial u/\partial z = 0$ at $z = h$. Multiplying the continuity equation, $\partial u/\partial r + u/r + \partial v/\partial z = 0$, by u, adding to (2.1) and integrating the result from $z = 0$ to $z = h$ leads to

$$\frac{1}{r}\frac{\mathrm{d}}{\mathrm{d}r}r\int_0^h u^2\mathrm{d}z = -gh\frac{\mathrm{d}h}{\mathrm{d}r} - ghs_b - \nu\left.\frac{\partial u}{\partial z}\right|_{z=0}. \tag{2.2}$$

In deriving this equation we have used the free-surface condition $\mathrm{d}h/\mathrm{d}r = (v/u)|_{z=h}$. Equation (2.1) can be used to find $h(r)$ provided some velocity profile across the fluid layer, $u(r, z)$, is assumed or derived. For simplicity, we make the same assumption as Tani, namely $u = U(r)(2z/h - z^2/h^2)$. More sophisticated profiles, such as the similarity solution of Watson (1964), can be used if necessary. Performing required integrations and using the mass conservation condition that the flow rate $Q = 2\pi r\int_0^h u\mathrm{d}z$ be constant, we arrive at Tani's equation modified by the inclusion of the slope function,

$$\frac{\mathrm{d}h}{\mathrm{d}r} = \left[\frac{3Q^2}{10\pi^2 g}\frac{1}{h^2r^3} - \left(s_b + \frac{3Q\nu}{2\pi g}\frac{1}{h^3r}\right)\right]\Big/\left(1 - \frac{3Q^2}{10\pi^2 g}\frac{1}{h^3r^2}\right), \tag{2.3}$$

Note that the denominator here is $1 - F^2$, where the effective Froude number squared, $F^2 = \overline{u^2}/gh = 3Q^2/(10\pi^2 gh^3r^2)$, is defined in terms of the mean-square velocity, $\overline{u^2} = (1/h)\int_0^h u^2\mathrm{d}z$. The flow divergence (the first term in the numerator of (2.3)) and the viscous damping (the third term in the numerator of (2.3)) have competing effects on the fluid depth and, depending on the sign of $1 - F^2$, tend to either increase or decrease the depth. Equation (2.3) describes the flow both ahead of and behind the jump. The reason that one must have a jump stems from the analysis of the critical points of (2.3), as will be shown below. At this point, we take the shock as given and formulate the jump conditions and the upstream conditions near the jet impact location.

From the continuity of mass and momentum fluxes across the jump, one finds that the flow depths on both sides of the jump are related through (see Bush & Aristoff 2003)

$$\frac{1}{2}\rho g\left(h_{2s}^2 - h_{1s}^2\right) + \sigma\zeta\frac{h_{2s} - h_{1s}}{r_j} = \int_0^{h_{1s}}\rho u^2\mathrm{d}z - \int_0^{h_{2s}}\rho u^2\mathrm{d}z, \tag{2.4}$$

where the subscript s denotes the jump state, 1 ahead of and 2 behind the jump, r_j is the jump radius and σ is the surface tension. The factor ζ is unity if the surface tension is accounted only in the jump region between the heights h_{1s} and h_{2s} (for a

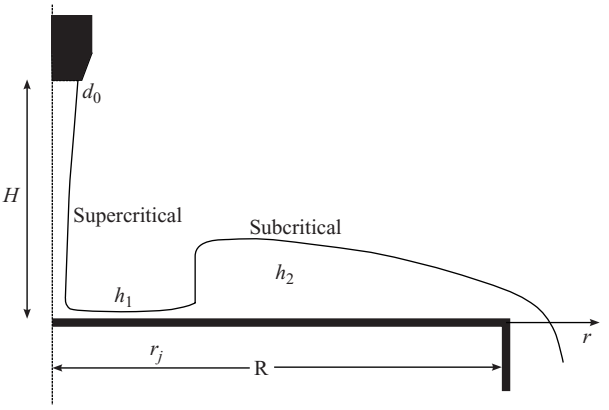

FIGURE 1. Schematic of the hydraulic jump experiment.

more accurate expression for ζ see § 4). The flow configuration is shown schematically in figure 1. Using the above ansatz for $u(r, z)$, we can find from this equation that

$$\frac{h_{2s}}{h_{1s}} = \frac{1}{2}\left(1 + \frac{2\zeta}{\bar{B}}\right)\left[-1 + \sqrt{1 + \frac{8F_{1s}^2}{(1 + 2\zeta/\bar{B})^2}}\right], \tag{2.5}$$

where $F_{1s}^2 = 3Q^2/(10\pi^2 g r_j^2 h_{1s}^3)$ is the effective Froude number squared just upstream of the jump and $\bar{B} = \rho g h_{1s} r_j/\sigma$. When surface tension is neglected, $\bar{B} \to \infty$, the jump condition (2.5) reduces to its familiar textbook form (White 2006).

The jump radius r_j is found from (2.5) as follows. Given the upstream condition near the jet impact point, i.e. $h_1(r_0)$ at some given r_0, one solves (2.3) to generate the upstream depth profile $h_1(r)$. With a unique downstream profile $h_2(r)$, one finds an r_j, such that at $r = r_j$, the solution profiles on both sides of the jump satisfy the jump condition (2.5). In order to generate the unique downstream profile, one needs to consider the far-field boundary condition as shown in § 3. The upstream initial condition is set based on the following assumptions. Suppose the jet originates from a nozzle of internal diameter d_0, located at height H above the plate as shown in figure 1. Assuming Bernoulli's equation (ignoring surface tension here), we can find the jet diameter and velocity near the impact point as $d_1 = d_0(1 + 2gH/U_0^2)^{-1/4}$ and $U_1 = U_0(1 + 2gH/U_0^2)^{1/2}$, where $U_0 = 4Q/\pi d_0^2$ is the velocity of the fluid at the nozzle exit. Next we assume that at $r = r_0$ the surface velocity, $U(r_0)$, is the same as U_1. Then the initial depth at r_0 is $h_0 = 3Q/(4\pi U_1 r_0)$ from mass conservation.

We now explain the importance of the additional ingredient in our formulation that was absent in previous analyses, the bottom topography $b(r)$, which is chosen to represent a plate of finite size. It is important from a physical standpoint that, if the outer edge is absent, i.e. the plate is assumed infinite, one should never expect to see a steady solution, as the outer depth will be increasing in time and hence the jump will be continuously pushed toward the jet. However, if the plate is sufficiently large, but finite, and fluid is sufficiently viscous, then the steady solution with a jump can exist. The inclusion of s_b has important mathematical consequences as well: the steady-state differential equation for h may posses several critical points whose existence, type, and location depend on the size and shape of the base plate as well as the flow conditions. Specifically, in addition to the spiral point responsible for the occurrence of a jump (see Bohr *et al.* 1993), there is also a saddle point near the plate edge, from which one can find a unique integral curve for the outer subcritical solution that provides a smooth transition of the solution from downstream subcritical flow

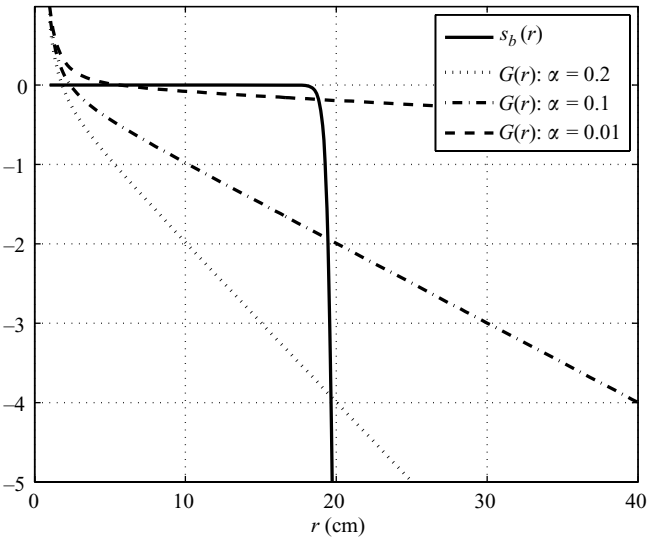

FIGURE 2. The curves $s_b(r)$ (3.3) and $G(r) = r^{-5/3} - \alpha r$. The intersections of s_b and G are the critical points of (3.4).

to supercritical flow over the edge. The problem of the lack of asymptotic states and of blow-up of downstream solutions, discussed in Bohr *et al.* (1993), is eliminated in this formulation.

3. Analysis of critical points

To understand the character of solutions of (2.3) we need to analyse the nature of its critical points. We first scale the variables h and r with respect to $l = (3Q^2/10\pi^2 g)^{1/5}$. Then (2.3) becomes

$$\frac{\mathrm{d}h}{\mathrm{d}r} = \frac{1/h^2r^3 - (s_b + \alpha/h^3 r)}{1 - 1/h^3 r^2}, \tag{3.1}$$

where it is understood that all the variables and parameters are now dimensionless. The viscous damping coefficient is $\alpha = 5\pi[3/(10\pi^2)]^{1/5}\nu/(Q^3 g)^{1/5}$. The critical points of (3.1) are the roots of the system $h^3r^2 = 1$, $1/(h^2r^3) - s_b(r) - \alpha/(h^3 r) = 0$, which depend on the specific form of $s_b(r)$. Eliminating $h = r^{-2/3}$ from these equations, we obtain

$$f(r) \equiv r^{5/3}(s_b(r) + \alpha r) - 1 = 0. \tag{3.2}$$

The number of critical points depends now on how many positive real roots equation (3.2) has. One point we make immediately is that if $s_b = 0$, there is only one root, $r_c = \alpha^{-3/8}$. To understand the general nature of the roots of (3.2), let us rewrite it as $s_b(r) = r^{-5/3} - \alpha r \equiv G(r)$. Note that the right-hand side of this equation is a monotonically decreasing function that crosses the r-axis at $r = \alpha^{-3/8}$. If the function $b(r)$ is to represent a plate, then $s_b = 0$ up to the edge of the plate, $r = R$, and drops down to a large negative value immediately after. As a result, $G(r)$ can cross $s_b(r)$ at two points: at $r_{c1} \approx \alpha^{-3/8}$, that is independent of what happens near the edge, and at $r_{c2} \approx R$ (since $G \sim -\alpha r$ at large r and crosses s_b near $r \approx R$, see figure 2).

To be more specific, we consider

$$s_b = -a[1 + \tanh((r - R)/w)] \tag{3.3}$$

in the following calculations, which is a reasonable representation of the slope of a plate of radius R if w is taken sufficiently small and a sufficiently large. One can show then that $b(r) = -a[r + w\ln(\cosh((r - R)/w)/\cosh(R/w))]$, and $b(r) \approx 0$ at $r < R$

Flow rate: $Q = 10\,\mathrm{cm}^3\,\mathrm{s}^{-1}$	Plate radius: $R = 20\,\mathrm{cm}$
Viscosity: $\nu = 0.01\,\mathrm{cm}^2\,\mathrm{s}^{-1}$	Plate-shape parameter: $w = 0.1\,\mathrm{cm}$
Density: $\rho = 1\,\mathrm{g\,cm}^{-3}$	Plate-shape parameter: $a = 10$
Nozzle height: $H = 2\,\mathrm{cm}$	Initial radius for $h_1(r)$: $r_0 = 1.2(d_1/2)$
Nozzle diameter: $d_0 = 0.8\,\mathrm{cm}$	Surface tension: $\sigma = 0$

TABLE 1. The basic parameter set (see figure 1 and (3.3) for definitions). Unless otherwise noted, these are the default parameters.

and $b(r) \approx 2a(R-r)$ at $r > R$. After making specific choices for the parameters a, w and R (see table 1) we can solve for the roots of (3.2) to find the critical points. Let (r_c, h_c) be a critical point, rewrite (3.1) as the dynamical system

$$\frac{\mathrm{d}h}{\mathrm{d}t} = h - \alpha r^2 - h^3 r^3 s_b, \quad \frac{\mathrm{d}r}{\mathrm{d}t} = h^3 r^3 - r, \tag{3.4}$$

and linearize (3.4) about (h_c, r_c) to obtain $\mathrm{d}\boldsymbol{u}/\mathrm{d}t = \boldsymbol{J}_c\boldsymbol{u}$, where $\boldsymbol{u} = (h, r)^T$ and $\boldsymbol{J}_c$ is the Jacobian at the critical point, whose eigenvalues are $\lambda_{1,2} = p(1 \pm \sqrt{1 - q/p^2})$, where $p = \frac{3}{2}(1 - r_c^{5/3} s_b)$ and $q = 8 + 3r_c^{5/3}(-s_b + r_c s_b')$. For reasonable bottom profiles, the eigenvalues at $r = r_{c1}$ are complex, hence r_{c1} is a spiral critical point, and at $r = r_{c2} \approx R$ they are real and of opposite sign, hence near the plate edge the critical point is a saddle.

4. Calculation of the jump radius

There are two main conclusions from the previous analysis. One is that it is impossible to have a spiral critical point in a smooth continuous flow, so there must be a discontinuity somewhere near the critical point that connects the integral curves approaching the point from either side (see Bohr *et al.* 1993; Tani 1949). The integral curve corresponding to the supercritical flow upstream is uniquely determined by the initial condition at $r = r_0$. The second conclusion concerns the uniqueness of the downstream integral curve: the unique integral curve must be the one that provides a saddle-point connection with the flow behind the saddle point. Thus the solutions on both sides of the jump can be uniquely determined and the downstream solution passes smoothly through the saddle point. The yet undetermined location of the jump is found from the jump condition (2.5). We give specific calculations next.

Define

$$\phi(r) \equiv \frac{h_2(r)}{h_1(r)} + \frac{1}{2}\left(1 + \frac{2\zeta}{B}\frac{1}{r h_1(r)}\right)\left[1 - \sqrt{1 + \frac{8}{r^2 h_1^3(r)}\left(1 + \frac{2\zeta}{B}\frac{1}{r h_1(r)}\right)^{-2}}\right], \tag{4.1}$$

which is (2.5) in terms of dimensionless variables. $B = \rho g l^2/\sigma$ is the Bond number. The jump radius r_j is the root of ϕ. To find h_1 and h_2 we integrate (3.4) once from $(h, r) = (h_0, r_0)$ to generate the upstream solution, $h_1(r)$, and once from $(h, r) = (h_{c2}, r_{c2})$, i.e. out of the saddle point towards $r < r_{c2}$, to generate the downstream solution, $h_2(r)$. These two solution profiles are terminated at turning points, where $\partial h/\partial r = \infty$, that are denoted by r_1 and r_2 (see figure 3). The hydraulic jump is located somewhere in the interval $[r_2, r_1]$. The plot of $\phi(r)$, with $r_2 < r < r_1$ shows that there is a unique point $r = r_j$ where the jump condition, $\phi = 0$, is satisfied; that point is the location of the hydraulic jump. The factor $\zeta = 1 + (s - \Delta r)/(h_{2s} - h_{1s})$ in (4.1) accounts for the surface tension force due to the part of the profile of h_2 from

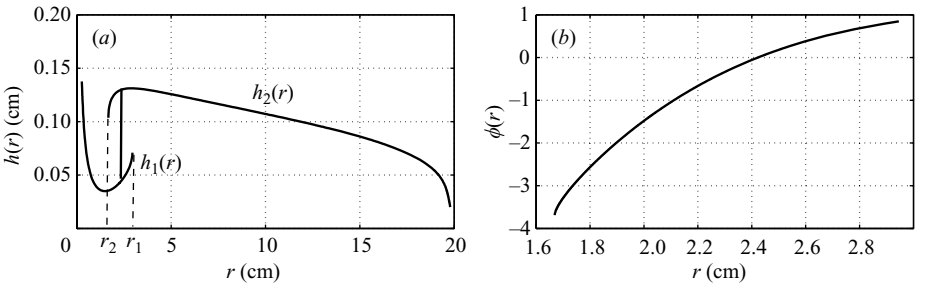

FIGURE 3. (*a*) The profiles of the upstream, h_1, and downstream, h_2, depths for the basic parameter set, table 1. (*b*) The profile of $\phi(r)$ for the same parameters. The vertical solid line in (*a*) shows the jump location where $\phi = 0$, while the dashed lines indicate the locations of the turning points.

$r = r_j$ to $r = r_1$ (see Bush & Aristoff 2003). Here s is the arclength of h_2 between r_j and r_1, which can be computed numerically, and $\Delta r = r_1 - r_j$. With this algorithm we can determine various dependences of r_j on the parameters of the problem, such as the flow rate Q, viscosity ν, surface tension σ and the plate radius R. In particular, figure 4(*a*) shows the dependence of the jump radius on the flow rate for parameters defined in table 1, which are chosen to be close to those of Bohr *et al.* (1993). One can see that the power law, $r_j \sim Q^p$, holds over a wide range of the values of Q with the exponent close to $p = 0.625$ of Bohr *et al.* (1993). However, the exponent depends in general on the surface tension σ, the plate radius, etc. In figure 4(*b*) we show the effect of the plate radius on both r_{c1} and r_j: the locus of the spiral critical point, r_{c1}, is essentially unaffected by R, while the effect of R on the jump radius is evident. Generally, our predictions with surface tension are in close agreement with the results of Bohr *et al.* (1993) at large Q, but at small Q the jump radius becomes substantially smaller than the prediction without surface tension. The jump indeed occurs close to the location of the first critical point if $\sigma = 0$, which to good accuracy is equal to $r_{c1} = \alpha^{-3/8}$ and this explains why the power law holds: since $\alpha = c_1 \nu Q^{-3/5} g^{-1/5}$ and the length scale is $l = c_2 Q^{2/5} g^{-1/5}$, it follows that in dimensional terms $r_j \approx r_{c1} l = c Q^{5/8} \nu^{-3/8} g^{-1/8}$ in agreement with Bohr *et al.* (1993).

Next we investigate the role of surface tension in more detail. Bush *et al.* (2006) have reported that reducing the surface tension by adding a surfactant may result in polygonal jumps relaxing to a circular jump of a slightly larger radius than the average radius of the polygonal jump. Thus the increase in surface tension is observed to have a destabilizing effect on the jump, possibly causing the transition from a circular to a polygonal shape. In qualitative agreement with these observations, we find that above a certain critical surface tension σ_c, the jump condition (4.1) has no solution. Thus, within the limitations of the present theory a steady circular hydraulic jump does not exist if the surface tension is too large. There must be a transition to either a circular, but unsteady jump, or a non-circular jump. Note that the jump may become unstable before the conditions for the non-existence of the steady-state solution are reached. In other words, the critical conditions we found are sufficient, but not necessary for the jump instability. The lack of solutions of (4.1) at large σ can be explained as follows. Large σ means small B and hence large values of $\xi = 1/2(1 + 2\zeta/Brh_1)$. Since the surface tension is included only in the jump conditions, the solution profiles $h_1(r)$ and $h_2(r)$ are unaffected by the change of σ. Now the jump condition (4.1) becomes $h_2 h_1^2 r^2 = 1/\xi + O(1/\xi^2)$ at $\xi \gg 1$ and this equation ceases to have solutions at ξ above a certain value, because h_2, h_1, and r vary within some fixed ranges (see figure 3*a*) independent of ξ and $h_2 h_1^2 r^2$ will be bounded from below by some positive number.

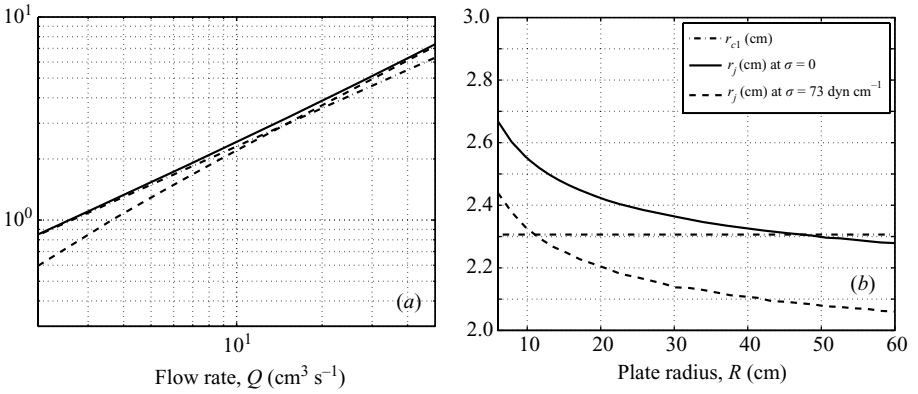

FIGURE 4. (*a*) Jump radius r_j, and the locus of the spiral critical point r_{c1}, which is the jump radius according to the power law of Bohr *et al.* (1993), as functions of the flow rate. (*b*) The jump radius r_j, and the locus of the spiral critical point r_{c1}, as functions of the plate radius R.

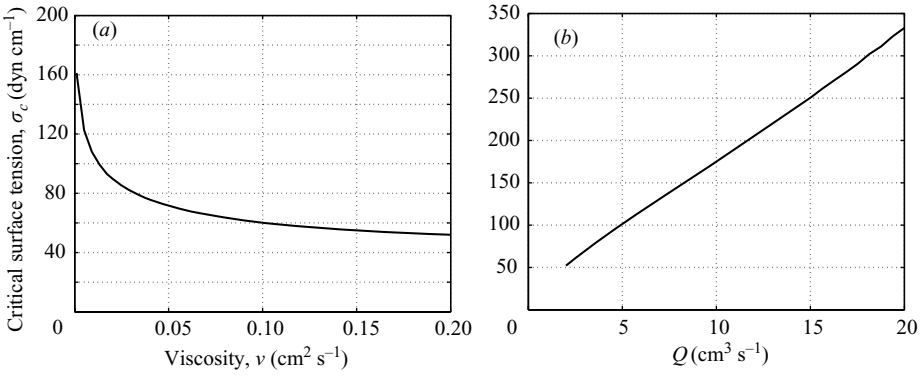

FIGURE 5. (*a*) The critical surface tension σ_c, as a function of viscosity ν, at $Q = 2\,\mathrm{cm}^3\,\mathrm{s}^{-1}$. (*b*) The critical surface tension vs flow rate at $\nu = 0.2\,\mathrm{cm}^2\,\mathrm{s}^{-1}$. In both cases, $a = 20$ (see table 1).

Physically, the reason for the existence of the critical surface tension is also clear: if the surface tension is too large, the change in the momentum flux across the jump will not be able to compensate for the surface tension force that tends to reduce the jump radius. At exactly the critical conditions, the jump is located at the turning point of $h_2(r)$, where $r^2 h_2^3 = 1$, $r = r_j$. Using this equation together with $\phi = 0$, we can find the critical Bond number as $B_c = 2\zeta/\{h_1 r_j[2(h_2/h_1)^2 - h_2/h_1 - 1]\}$, and the critical surface tension as $\sigma_c = \rho g l^2/B_c$, where $h_2 = r_j^{-2/3}$, $h_1 = h_1(r_j)$. In figure 5(*a*) we plot the dependence of the critical surface tension σ_c, on the fluid viscosity ν. As we can see, σ_c decreases rapidly with increasing ν. This trend is in accord with experiment in the sense that the polygonal jumps are only observed in highly viscous fluids (see Ellegaard *et al.* 1998, 1999; Bush *et al.* 2006). Higher flow rates tend to increase σ_c as well, as shown in figure 5(*b*).

5. Discussion

Our model builds on the work of Tani (1949), Bohr *et al.* (1993) and Bush & Aristoff (2003) with two main goals: (i) to develop a theory of a steady-state circular jump that can provide a base-state solution for the analysis of the jump instability; (ii)

to eliminate some of the ambiguities that remained in previous analyses, in particular the issue of the far-field singularities of solutions of the averaged equations.

Hydrodynamic stability analysis always requires that a base-state solution be known. Previous analyses of the steady hydraulic jump were restricted primarily to the flow upstream of the jump, while the details of the downstream flow were relegated to an empirical input, such as the downstream depth (Watson 1964). This is unsatisfactory because the flow downstream of the jump is subcritical and therefore determines the state behind the jump which in turn determines the jump radius. The steady-state solution developed here can be used as a base-state solution for the stability analysis of the hydraulic jump, currently underway. Our finding that the steady-state circular jump does not exist if the surface tension exceeds a certain critical value underscores the important role the surface tension may play in the onset of the instability.

The unphysical aspect of the model of Tani (1949) and Bohr *et al.* (1993) of the lack of asymptotic solutions at large r is removed in our formulation by a careful consideration of the boundary condition at the edge of the plate. A saddle point that exists now near the edge of the plate allows determination of a unique and regular solution downstream of the jump that can connect smoothly with the flow over the plate edge.

The hydraulic jump in the present formulation is an example of a shallow-water transcritical flow. There exists related literature in hydraulics theory where various problems of flows over topography (e.g. flow over a sill) are considered (see e.g. Garrett 2004). Similar to our study, the nature of the critical point (called a 'control point' in hydraulics) over a sill plays a key role in determining the solutions of the shallow-water equations. However, we next discuss a rather unexpected gasdynamic analogue of the circular hydraulic jump – a detonation wave. The basic model of a steady planar detonation wave in an ideal gas is called the ZND (Zel'dovich–von Neumann–Döring) model (see Fickett & Davis 1979). The detonation wave represents a shock wave that propagates in a medium where exothermic chemical reactions release thermal energy if the medium is sufficiently heated. The reactions sustain the shock and the shock in turn keeps the temperature high enough to sustain the chemical reactions. Thus it is possible to have a self-sustained wave that propagates at a constant speed, say D. The basic question of detonation theory is: given a reactive mixture with specified thermodynamic and chemical properties, how does one find the detonation speed?

The flow structure of a one-dimensional detonation wave is shown in figure 6. Across the reaction zone, the mass, momentum, and energy fluxes are conserved: $\rho U = \rho_a D$, $p + \rho U^2 = p_a + \rho D^2$ and $e + p/\rho + U^2/2 = e_a + p_a/\rho_a + D^2/2$, where p, ρ, U are the pressure, density and flow speed, respectively, $e = p/(\gamma - 1)\rho - \lambda q$ is the internal energy of the gas that includes also the chemical part, λq, λ is the reaction progress variable that is 0 before the reaction starts, 1 if all fuel is consumed and takes intermediate values during the chemical reaction, q is the heat of reaction per unit mass of the mixture and γ is the ratio of specific heats. The subscript a indicates the ambient state ahead of the shock. These three equations can be solved for p, ρ and U in terms of the reaction-progress variable λ, but importantly, D is yet undetermined. How does one find D? The key to this question is that the speed is determined by what happens in the subsonic reaction zone because the reaction zone is causally connected to the shock. Therefore, one must consider the state of the reaction zone and find an additional equation that would determine D. If the detonation wave is self-sustained (Chapman–Jouguet detonation, see Fickett & Davis 1979), it is characterized by the reaction zone having a trailing sonic point that is the boundary of the subsonic region. The existence of the sonic point immediately leads

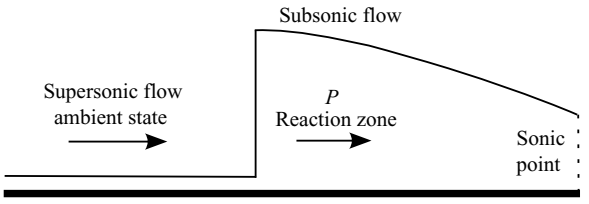

FIGURE 6. The pressure profile in detonation: supersonic flow enters the shock and becomes a subsonic flow that accelerates to the sonic condition at the end of the reaction zone.

to a unique value of D which is found from the sonic condition, $U = c$ (c is the local sound speed) at the end of the reaction zone, $\lambda = 1$. Specifically, since $c = \sqrt{\gamma p/\rho}$, the equation $U(\lambda, D) - (\gamma p(\lambda, D)/\rho(\lambda, D))^{1/2} = 0$ at $\lambda = 1$ yields the detonation speed, D.

So, just as in detonation theory the detonation speed is determined by the critical conditions at the end of the subsonic region, the jump radius is uniquely determined by the critical conditions at the end of the subcritical region behind the hydraulic jump. The analogy sheds light on the nature of the hydraulic-jump problem both from a physical standpoint and its mathematical formulation. Of course, unlike the detonation wave, the hydraulic jump involves additional complications, such as the finite extent and complex internal structure of the jump region and the surface tension that will raise more issues to be addressed in the future. The analogy can be explored further and may help us understand some of the complex structures that exist in both of these phenomena. In particular, it is well-known in detonation theory that detonation shocks tend to be unstable and develop cellular structures (see Fickett & Davis 1979), strikingly similar to the polygons in the hydraulic jumps (see Ellegaard *et al.* 1998).

The author thanks Professors John Bush and Ruben Rosales of MIT for helpful discussions.

REFERENCES

BOHR, T., DIMON, P. & PUTKARADZE, V. 1993 Shallow-water approach to the circular hydraulic jump. *J. Fluid Mech.* **254**, 635–648.

BUSH, J. & ARISTOFF, J. 2003 The influence of surface tension on the circular hydraulic jump. *J. Fluid Mech.* **489**, 229–238.

BUSH, J., ARISTOFF, J. & HOSOI, A. 2006 An experimental investigation of the stability of the circular hydraulic jump. *J. Fluid Mech.* **558**, 33–52.

ELLEGAARD, C., HANSEN, A. E., HAANING, A., HANSEN, K., MARKUSSEN, A., BOHR, T., HANSEN, J. L. & WATANABE, S. 1998 Creating corners in kitchen sinks. *Nature* **392**, 767–768.

ELLEGAARD, C., HANSEN, A. E., HAANING, A., HANSEN, K., MARKUSSEN, A., BOHR, T., HANSEN, J. L. & WATANABE, S. 1999 Cover illustration: Polygonal hydraulic jumps. *Nonlinearity* **12**, 1–7.

FICKETT, W. & DAVIS, W. C. 1979 *Detonation*. Berkeley, CA: University of California Press.

GARRETT, C. 2004 Frictional processes in straits. *Deep-Sea Res.* II **51**, 393–410.

GILMORE, F. R., PLESSET, M. S. & CROSSLEY JR, H. E. 1950 The analogy between the hydraulic jumps in liquids and shock waves in gases. *J. Appl. Phys.* **21**, 243–249.

KATE, R. P., DAS, P. K. & CHAKRABORTY, S. 2007 Hydraulic jumps due to oblique impingement of circular liquid jets on a flat horizontal surface. *J. Fluid Mech.* **573**, 247–263.

RAYLEIGH, LORD 1914 On the theory of long waves and bores. *Proc. R. Soc. Lond.* A **90**, 324.

STOKER, J. J. 1957 *Water Waves*. Interscience.

TANI, I. 1949 Water jump in the boundary layer. *J. Phys. Soc. Japan* **4**, 212–215.

WATSON, E. J. 1964 The radial spread of liquid jet over a horizontal plane. *J. Fluid Mech.* **20**, 481–499.

WHITE, F. 2006 *Fluid Mechanics*. McGraw-Hill.